



ORIGINAL ARTICLE

A simple method for the simultaneous encapsulation of ciprofloxacin into PEGDA/alginate hydrogels using gamma irradiation



Farah Nurlidar ^{a,*}, Dien Puji Rahayu ^a, Deudeu Lasmawati ^a, Ade Lestari Yunus ^a, Rika Heryani ^b, Nani Suryani ^b

^a Research Center for Radiation Processing Technology, Research Organization for Nuclear Energy, National Research and Innovation Agency, Jakarta, Indonesia

^b Deputy for Infrastructure Research and Innovation, National Research and Innovation Agency, Jakarta, Indonesia

Received 13 December 2022; accepted 5 March 2023

Available online 15 March 2023

KEYWORDS

3D scaffold;
Poly(ethylene glycol) diacrylate;
Alginate;
Ciprofloxacin;
Simultaneous drug encapsulation;
Gamma-irradiation

Abstract Herein, we present a simple simultaneous method for the fabrication of poly(ethylene glycol) diacrylate/alginate (PEGDA/ALG) hydrogels as three-dimensional (3D) scaffolds for ciprofloxacin (CIP) encapsulation using gamma-irradiation at an irradiation dose of 15 kGy. The absorption capacity of the hydrogels studies demonstrated that the PEGDA/ALG hydrogels showed a small absorption capacity at an acidic pH (pH = 2) and a high absorption capacity at a basic pH (pH = 10). The morphology and functional groups of the PEGDA/ALG hydrogels were successfully determined using scanning electron microscopy (SEM) and fourier transform infrared spectroscopy (FT-IR), respectively. SEM images observed a decrease in the pore size of the hydrogels with increasing alginate concentration, indicating successful alginate incorporation. FT-IR spectra of the hydrogels indicated that the PEGDA and alginate were crosslinked. The antimicrobial experiment showed that all the PEGDA/ALG hydrogels possessed good antimicrobial activity against Gram-positive bacteria (*Staphylococcus aureus*) and Gram-negative bacteria (*Escherichia coli*). These results demonstrate the practicality and efficacy of gamma-irradiation as a one-step method for the simultaneous fabrication of PEGDA/ALG hydrogels and encapsulation of CIP without compromising the bioactivity of the encapsulated CIP.

© 2023 The Author(s). Published by Elsevier B.V. on behalf of King Saud University. This is an open access article under the CC BY-NC-ND license (<http://creativecommons.org/licenses/by-nc-nd/4.0/>).

* Corresponding author at: Research Center for Radiation Processing Technology, Research Organization for Nuclear Energy, National Research and Innovation Agency, Jl. Lebak Bulus Raya No. 49, Jakarta Selatan 12440, Indonesia.

E-mail address: farah.nurlidar@brin.go.id (F. Nurlidar).

Peer review under responsibility of King Saud University.



1. Introduction

Hydrogels, three-dimensional (3D) cross-linked polymeric networks, have been proven to regulate the delivery of bioactive molecules, including low molecular weight drugs, nucleic acids, and proteins due to their unique structural and functional properties (Li & Mooney, 2016; Liu et al., 2017; Mahmood et al., 2022).

The enhancement of hydrogels' properties can be reinforced through both physical and chemical crosslinking techniques (Das et al., 2018; Liu et al., 2017). Hydrogels formed by chemical crosslinking techniques exhibit more stable structures that enable to give protection to drugs from harsh environments, such as low pH and enzymes in the stomach (Li & Mooney, 2016; Mantha et al., 2019; Zhang et al., 2020). However, this technique utilizes chemical crosslinking reagents, which may cause toxicity. Thus, to address the limitation, gamma rays can be applied to fabricate hydrogels in the absence of any chemical crosslinking reagents (Darwis et al., 2015; Fekete et al., 2017; Mantha et al., 2019). Moreover, the strategy using gamma rays offers great promise as the hydrogel fabrication and encapsulating drugs work concomitantly and escalate the drug-loading efficiency (El-Bagory et al., 2010; Masyruroh et al., 2020). A previous study reported that the drug encapsulation step runs after hydrogel fabrication resulting in low efficiency and a time-consuming process of drug-loading (Bustamante-Torres et al., 2021; Hanna & Saad, 2019; Wang et al., 2017).

Hydrogels can be synthesized from synthetic polymers (e.g. poly(ethylene glycol) (PEG), poly(methyl methacrylate) (PMMA), poly(acrylamide), poly(2-hydroxyethyl methacrylate) (pHEMA), and poly(acrylic acid)) and/or natural polymers (alginate, bacterial cellulose, chitosan, dextran, and gelatin) (Bakaic et al., 2015; Nho et al., 2015; Nurlidar et al., 2017, 2022; Park et al., 2020; Tomić et al., 2007). Among these synthetic polymers, PEG has been extensively used as matrices for controlled drug delivery because of its excellent biocompatibility and low cytotoxicity (Ailincai et al., 2021; Bignotti et al., 2021; D'souza & Shegokar, 2016; Henise et al., 2015; Masyruroh et al., 2020). However, PEG is an inert polymer, which limits its ability to sustain control drug delivery. Hydrogel based on a combination of synthetic and natural polymers can be utilized to enhance the functionality and sustain the drug delivery ability of the hydrogels.

Alginate is one of the most naturally abundant and renewable polymers that has been extensively used for drug delivery systems. In this study, we developed gamma-irradiated PEGDA/alginate (PEGDA/ALG) hydrogels that can simultaneously encapsulate drug molecules into the hydrogels in a single-step process. We hypothesized that the PEGDA/ALG hydrogel would be suitable as a 3D scaffold for drug delivery systems due to its ease of fabrication and its capability in controlling drug release. Ciprofloxacin (CIP) is used as a drug model to investigate the capability of the PEGDA/ALG hydrogel to serve as a 3D scaffold for simultaneous drug encapsulation.

2. Materials and methods

2.1. Materials

PEGDA (average Mn 575) and CIP were purchased from Sigma-Aldrich (St Louis, MO, USA). Sodium alginate

(300–400 cP) was obtained from Wako Pure Chemical Industries Ltd. (Osaka, Japan). Buffer pH 2 and pH 10 solutions were ordered from Merck KGaA (Darmstadt, Germany). Nutrient agar (NA) was purchased from Difco Laboratories (Becton, Dickinson and Company, Sparks, MD, USA). All reagents were analytical grade and used without any additional processing.

2.2. Fabrication of PEGDA and PEGDA/ALG hydrogels

PEGDA and PEGDA/ALG hydrogels were fabricated by mixing CIP, PEGDA, and alginate homogeneously. Briefly, CIP (0.0273 g) was dissolved completely in 36 mL of hydrochloride solution (0.01 N). Four milliliters of PEGDA and sodium alginate (0–2% w/v) were then added to the CIP solution and mixed homogeneously. Four hundred microliters aliquot of the mixture solution was then dropped into a well in a 48-well tissue culture plate (Corning Incorporated, Corning, NY, USA) and irradiated using gamma rays (cobalt-60; Gamma Cell 220 Upgraded, Izotop, Hungaria) at irradiation dose of 15 kGy (dose rate = 4.8 kGy/hours). The final concentrations of CIP, PEGDA, and sodium alginate in the solution are presented in Table 1.

The obtained hydrogels were freeze-dried and weighed to obtain the weight of the dried gel. The dried gels were then immersed in 5 mL of demineralized water and incubated in a shaking incubator at 37 °C and 60 rpm for 24 h. The hydrogels were then washed three times with demineralized water to remove unreacted polymers and freeze-dried. Gel fraction was calculated, as defined by:

$$\text{Gel fraction (\%)} = \frac{\text{Weight of the dried gel after washing}}{\text{Weight of the dried gel before washing}} \times 100 \quad (1)$$

The absorption capacity of the hydrogels was carried out by immersing the dried gel in 5 mL of buffer pH 2 or phosphate-buffered saline (Dulbecco's PBS; pH 7.4) or buffer pH 10 solution at 37 °C for 24 h. The absorption capacity was calculated as follows:

$$\begin{aligned} \text{Absorption capacity (\%)} \\ = \frac{\text{Weight of wet gel} - \text{weight of dried gel}}{\text{Weight of dried gel}} \times 100 \end{aligned} \quad (2)$$

2.3. Characterization of PEGDA and PEGDA/ALG hydrogels

The fourier transform infrared (FT-IR) spectra of the freeze-dried hydrogels were recorded in the range 400–4000 cm⁻¹ using a Prestige-21 FT-IR spectrometer (Shimadzu, Kyoto,

Table 1 The final concentration of CIP, PEGDA, and sodium alginate in the solution for hydrogel fabrication.

Sample	PEGDA (% v/v)	Sodium alginate (% w/v)	CIP (mg/mL)	Irradiation dose (kGy)
PEGDA	10	0	0.6825	15
PEGDA/ALG 0.5%	10	0.5	0.6825	15
PEGDA/ALG 1.0%	10	1	0.6825	15
PEGDA/ALG 2.0%	10	2	0.6825	15

Japan) based on the KBr method with 45 scans and a resolution of 2 cm^{-1} .

Morphology of the freeze-dried gels was observed under low vacuum conditions using a scanning electron microscope (SEM; Quanta 650; Thermo Fischer, Massachusetts, USA) at an acceleration voltage of 10 kV without gold coating.

An unconfined compression test of the hydrogels was conducted on a universal testing machine (Zwick Roell; Z005, Ulm, Germany) with a load cell of 20 N and a test speed of 20 mm/min. The cylindrical shape freeze-dried gels (5 mm in height and 9 mm in diameter) were tested in their swollen state after 24 h of incubation of the freeze-dried gels in PBS. The compression was performed up to 70% of sample deformation. The elastic modulus of the hydrogels was calculated using the slope of stress–strain curves with compressive strains ranging from 0.5 to 5%. The data was processed with the test Xpert III (Zwick Roell) software.

2.4. *In vitro* release of CIP from PEGDA and PEGDA/ALG hydrogels

The stability of the CIP after gamma-irradiation was evaluated using the UV/visible spectrophotometer (UV/Vis, Cary 100, Agilent, California, USA) by comparing the spectra of CIP released from the hydrogel and CIP solution in PBS.

In vitro release studies of CIP from freeze-dried PEGDA and PEGDA/ALG hydrogels were carried out by incubating each hydrogel in 5 mL of the PBS medium at 37 °C with agitation (60 rpm). At the predetermined time, all supernatant in the tube was taken out and replaced with the same amount of PBS medium to maintain the same volume of the release medium in the tube. The concentration of the released drug (CIP) was determined by UV/Vis spectrophotometer and calculated using a calibration curve of CIP solution in PBS. The same procedure was repeated with buffer pH 2 and 10.

$$\text{CIP release (\%)} = \frac{\text{Amount of CIP release}}{\text{Total CIP in the hydrogel}} \times 100 \quad (3)$$

2.5. *In vitro* antibacterial activity of PEGDA and PEGDA/ALG hydrogels containing CIP

Antibacterial activity against *Escherichia coli* (*E. coli*; Food and Nutrition Culture Collection (FNCC) 0091, Gadjah Mada University) and *Staphylococcus aureus* (*S. Aureus*; FNCC 0047) of the PEGDA and PEGDA/ALG hydrogels containing CIP was investigated using a double-layer diffusion method. A double-layer (base and seed layers) of NA medium was prepared for the antibacterial activity test. The base layer was prepared by pouring 20 mL of warm sterilized NA medium onto the sterilized glass Petri dished ($d = 14\text{ cm}$). The NA medium was then allowed to solidify at room temperature and kept overnight at 37 °C. The bacteria suspension was prepared in sterilized demineralized water and the concentration of the bacteria was determined by the total plate count method. The seed layer was prepared by pouring 20 mL of warm sterilized NA medium containing bacteria at a concentration of about 10^7 CFU/mL onto the surface of the base layer and kept at room temperature on a clean bench for 30 min. The PEGDA and PEGDA/ALG hydrogels containing CIP (the amount of CIP was $51.19\text{ }\mu\text{g}$ per hydrogel) were then placed

on the surface of the seed layer. The inhibition zones of bacterial growth around the hydrogels were measured after incubation for 24 h at 37 °C.

2.6. Statistical analysis

All statistical analyses were carried out using the one-way analysis of variance routine of KaleidaGraph 4.5 (Synergy Software, Reading, PA, USA) followed by Tukey's honestly significant difference test. A value of $p < 0.05$ was accepted as statistically significant. All data are presented as mean \pm standard deviation, with $n = 3$.

3. Results and discussion

3.1. Fabrication of PEGDA and PEGDA/ALG hydrogels

Simultaneous encapsulation of CIP into PEGDA and PEGDA/ALG hydrogels was successfully conducted by radiation crosslinking using gamma rays of the homogeneous solution containing PEGDA, sodium alginate, and CIP. During gamma ray exposure, the radical processes in an aqueous solution are primarily initiated by the reactive intermediates such as hydrated electrons, hydroxyl radicals, and hydrogen atoms, that formed because of water radiolysis (Jonah et al., 1990; Mantha et al., 2019). The reactive intermediates may react with the PEGDA and alginate to form macroradicals that can crosslink each other to form an insoluble 3D polymeric structure. In addition, alginate may also undergo degradation during gamma exposure due to direct chain scission of glycosidic linkage by the reactive intermediates (Nagasawa et al., 2000).

To investigate the amount of the crosslinked fraction of the polymers in the hydrogel, a gel fraction experiment was performed. A gel fraction value indicates the proportion of the polymers in the hydrogel compared to their initial amounts before hydrogel formation (Nurlidar et al., 2017). Gel fraction studies of the PEGDA and PEGDA/ALG hydrogels showed that changing alginate concentration in the range of 0–2.0% influenced the gel fraction of the hydrogels significantly ($p < 0.0001$) (Fig. 1). PEGDA hydrogel without alginate showed the highest gel fraction ($96.14 \pm 1.37\%$), while PEGDA/ALG 2.0% showed the fewest gel fraction ($86.52 \pm 0.33\%$). At a high concentration of alginate, the crosslinking reaction was hindered by low polymer chain mobility because of the high viscosity of the polymer solution. As a result, at high alginate concentrations, radiation-induced alginate degradation prevails, as evidenced by the hydrogel's low gel fraction. The previous report showed that crosslinking reaction between the macroradicals is influenced by the mobility of the polymer chains and the distance between the neighbouring macroradicals (Fekete et al., 2017).

Absorption capacity is a key factor for investigating hydrogels for drug delivery systems because it regulates the release of the encapsulated drug from the hydrogels (Liu et al., 2017). In this work, the absorption capacity of freeze-dried hydrogels was conducted at three different pH values, which are pH = 2, PBS (pH = 7.4), and pH = 10. After 24 h, the results showed that all hydrogels showed little absorption capacity in acidic pH (pH = 2) due to the carboxyl groups in the alginate structure being protonated (COOH), while they showed high

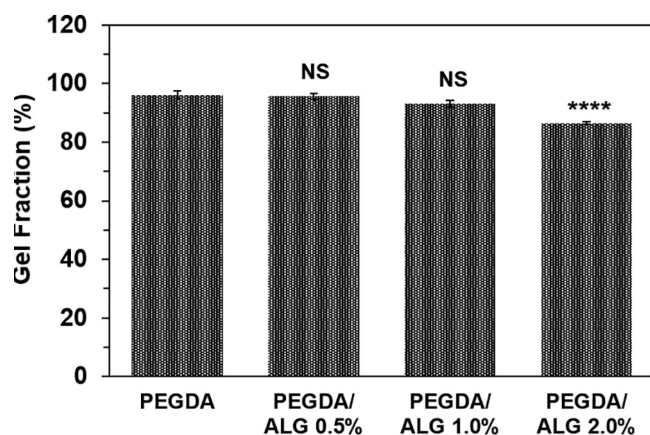


Fig. 1 Gel fraction of the PEGDA and PEGDA/ALG hydrogels (**** $p < 0.0001$ and NS = not significant compared to PEGDA hydrogel).

absorption capacity at basic pH (pH = 10) as the carboxyl groups were in an anionic state (COO^-) (Fig. 2). It has been reported that hydrogels containing ionizable groups such as carboxyl or amine are sensitive to environmental changes and may swell during ionization (Mahmood et al., 2022). Therefore, there is an electrostatic repulsion between the carboxyl groups in the PEGDA/ALG hydrogels, which may cause 3D network swelling and then water absorption. These results indicated that the PEGDA and PEGDA/ALG hydrogels were sensitive to pH, which makes the hydrogels a good candidate for CIP delivery. The pH-responsive hydrogels for oral drug delivery have been proven to enhance the stability of drug delivery in the stomach and achieve controlled release in the intestines (Dahri et al., 2021; Khan et al., 2021; Liu et al., 2017; Rizwan et al., 2017).

Furthermore, Fig. 2 confirmed that the presence of alginate in the PEGDA hydrogel affected its absorption capacity. An increase in the alginate content resulted in an increase in

hydrogel absorption capacity due to the hydrophilicity of the alginate. However, the absorption capacity decreased as the alginate concentration was increased further. These results may be caused by differences in hydrogel crosslinking density. As the amount of alginate increases, the amount of polymeric network space that is available to absorb water is reduced. Other studies have found that the density of the polymeric network affects the absorption capacity of the hydrogels (Nurlidar et al., 2018; Zang et al., 2022).

SEM images of the freeze-dried PEGDA and PEGDA/ALG hydrogels are shown in Fig. 3. The images of PEGDA and PEGDA/ALG hydrogels show clear differences in their microstructures. The image of the PEGDA hydrogel (Fig. 3A) shows an irregular structure, while the images of PEGDA/ALG hydrogels (Fig. 3B-D) show interconnected pore structures with various pore sizes. Notably, it can be clearly seen in Fig. 3B-D that the pore diameter of the PEGDA/ALG hydrogels decreases as the alginate concentration increases. The difference in the pore size in the hydrogel structure is presumably because of the difference in the hydrogel crosslinking density. The higher the concentration of alginate in the hydrogel, the higher the crosslinking density. It has been reported that the pore size in the hydrogel network is proportional to crosslinking density and the size of the ice particles during the freeze-drying process (Yoo et al., 2004). These results suggest that there were interactions between the PEGDA and alginate polymers to form an interconnected network structure and are in agreement with the gel fraction analyses, in which almost all the polymers form a gel structure.

To further confirm the hydrogel behavior under a stress, a compression test of the hydrogel was conducted (Fig. 4A). The compressive stress of the PEGDA and PEGDA/ALG hydrogels at a deformation of 40% is shown in Fig. 4B. Compressive experimental results show that the PEGDA/ALG 2.0% has the highest compressive stress at 40% strain ($p < 0.0001$). The elastic modulus of the hydrogels presented in Table 2 demonstrated that the elastic modulus of the hydrogels significantly increased as the amount of alginate increased. The

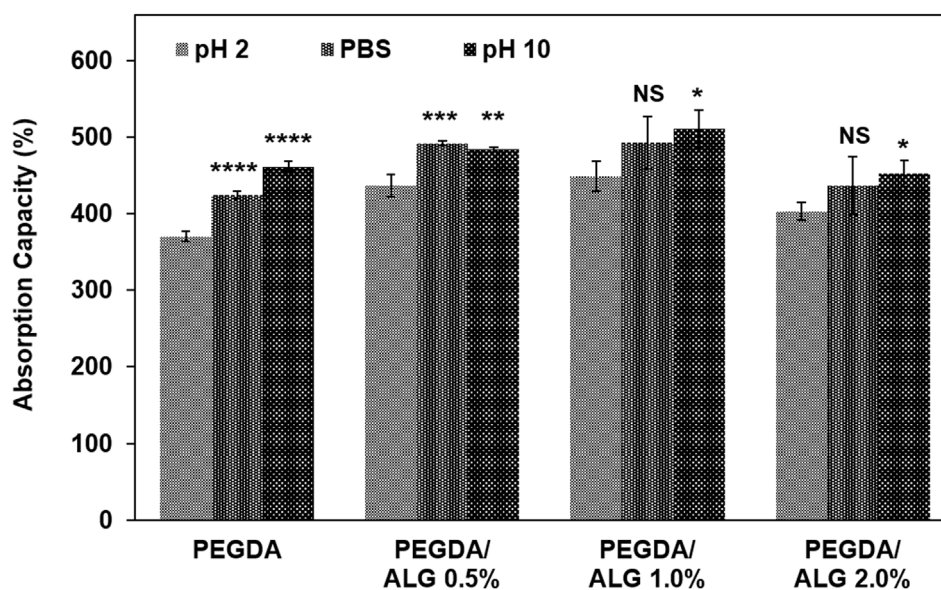


Fig. 2 The absorption capacity of the PEGDA and PEGDA/ALG hydrogels (* $p < 0.05$; ** $p < 0.01$; *** $p < 0.001$; **** $p < 0.0001$; and NS = not significant compared to the absorption capacity of the hydrogel at pH 2).

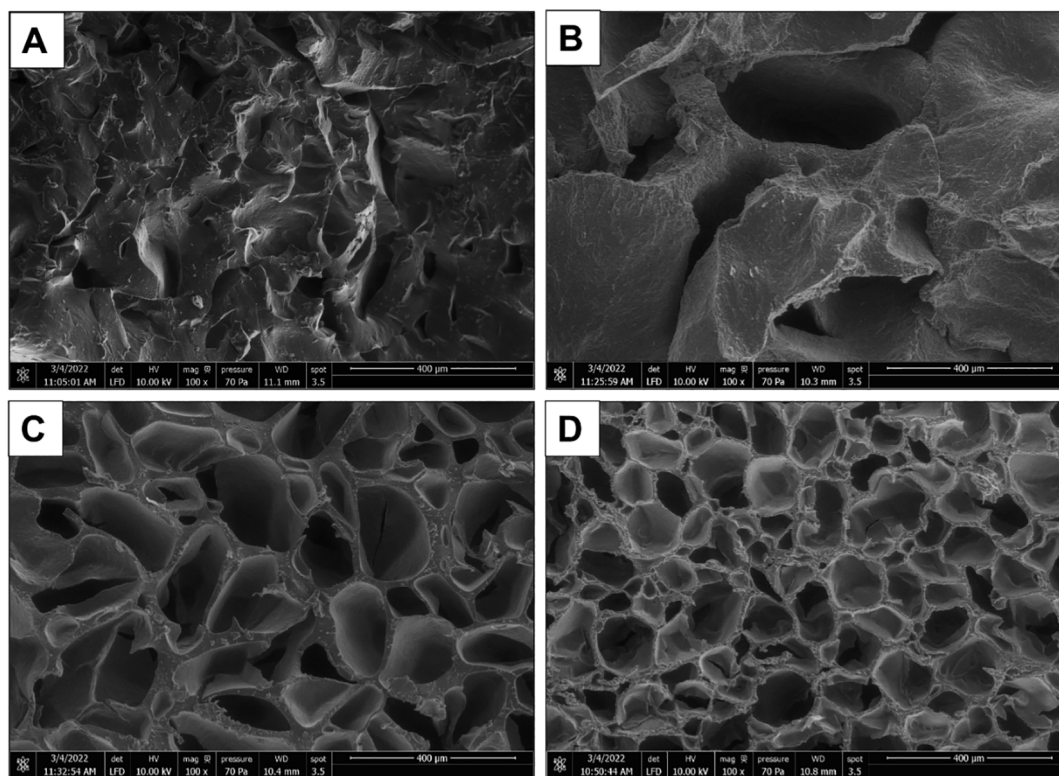


Fig. 3 SEM images of the freeze-dried PEGDA (A), PEGDA/ALG 0.5% (B), PEGDA/ALG 1.0% (C), and PEGDA/ALG 2.0% (D) hydrogels.

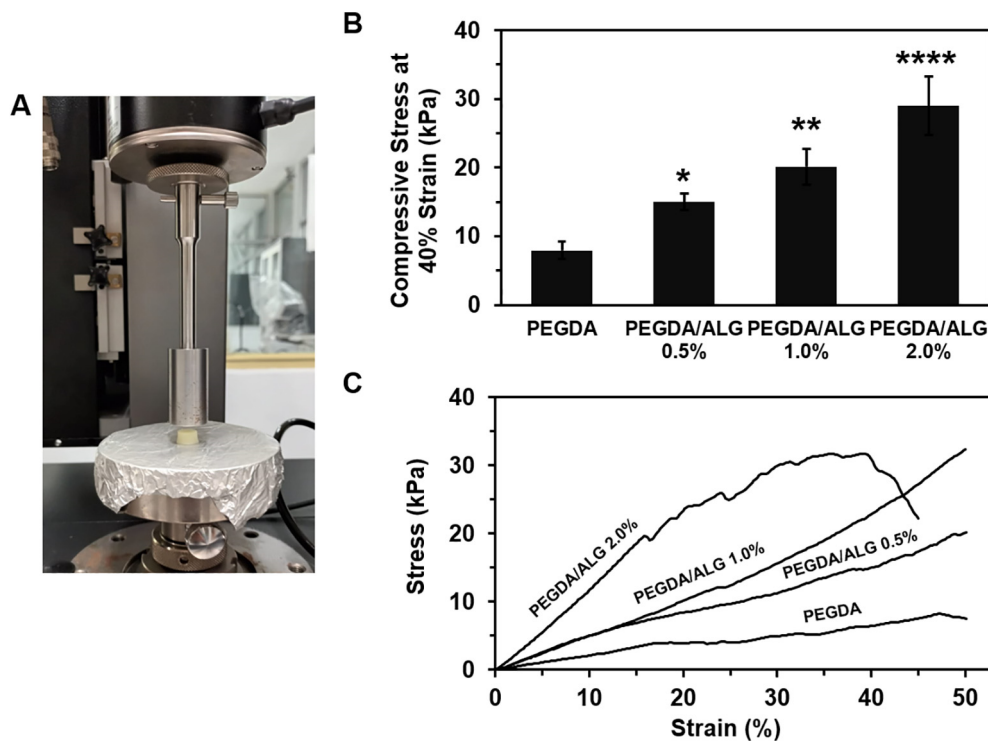


Fig. 4 The compressive test measurement (A), the compressive stress at 40% strain (B), and stress–strain curves (C) of PEGDA and PEGDA/ALG hydrogels (* $p < 0.05$; ** $p < 0.01$; and **** $p < 0.0001$ compared to PEGDA hydrogel).

Table 2 Elastic modulus of the PEGDA and PEGDA/ALG hydrogels.

Sample	Elastic modulus (kPa)	R ²
PEGDA	23.441 ± 1.345	0.9917
PEGDA/ALG 0.5%	49.153 ± 4.625 ****	0.9998
PEGDA/ALG 1.0%	51.380 ± 1.352 ****	0.9999
PEGDA/ALG 2.0%	109.505 ± 2.571 ****	0.9987

**** $p < 0.0001$ compared to PEGDA hydrogel.

PEGDA/ALG 2% hydrogels showed the highest elastic modulus compared to other hydrogels ($p < 0.0001$). These results suggest that increasing alginate concentration significantly increases the mechanical properties of the hydrogels, indicating that the alginate concentration plays an important role in the strength of the hydrogels. However, the stress-strain curves indicated that the PEGDA/ALG 2.0% was easily broken when subjected to large deformation compared to those hydrogels with lower alginate content (Fig. 4C). These results were due to the high crosslinking density between the polymeric chains in the PEGDA/ALG 2.0% hydrogel. It is well understood that gamma-irradiation of the polymer will cause chemical bond formation between the polymers, resulting in the formation of a rigid hydrogel network. It has been reported that a large number of chemical cross-links cause brittleness of the polyacrylamide hydrogels because the extension of the polymer chains is inhibited (Norioka et al., 2021).

To confirm the functional groups in the hydrogels, FT-IR measurement was conducted. FT-IR spectra of the sodium alginate, PEGDA monomer, and PEGDA and the PEGDA/ALG hydrogels are shown in Fig. 5A-F. It can be seen from Fig. 5A that the absorption peak at 1601 cm^{-1} was due to the asymmetric stretching vibration of COO^- in the sodium alginate. In the FT-IR spectrum of the PEGDA monomer, the peak at 1731 cm^{-1} is attributed to the C = O stretching in the PEGDA structure (Fig. 5B).

The FT-IR spectra of the PEGDA/ALG hydrogels (Fig. 5D-F) showed peaks at 1731 and 1601 cm^{-1} which were

assigned as C = O stretching in the PEGDA structure and COO^- asymmetric stretching in the sodium alginate, respectively. These results suggested the presence of both PEGDA and alginate in the PEGDA/ALG hydrogels, indicating the crosslinking formation between the PEGDA and alginate.

The evidence for the crosslinking formation between PEGDA and alginate can also be seen from the absorption peak around 3400–3600 cm^{-1} . Compared with the FT-IR spectrum of PEGDA hydrogel (Fig. 5C), it can be seen that –OH stretching vibration absorption peak of the PEGDA/ALG hydrogels at around 3400–3600 cm^{-1} was broadened and shifted to lower wavenumber (Fig. 5D-F). These results indicated that there is a strong intermolecular interaction between the polymers in the PEGDA/ALG hydrogels. In addition, as the alginate concentration increases, the asymmetric stretching absorption peak of the carboxyl group at 1601 cm^{-1} also broadens, indicating the strong interactions between the alginate and the PEGDA in the PEGDA/ALG hydrogels.

In addition, the distinct peaks that appeared at 1408 and 810 cm^{-1} (Fig. 5B) were assigned to acrylate double bonds ($\text{CH}_2 = \text{CH}$) in the PEGDA monomer (Visentin et al., 2014), and these peaks disappeared in the FT-IR spectra of PEGDA and PEGDA/ALG hydrogels (Fig. 5C-F). The disappearance of these peaks may confirm the conversion of the C = C double bond in the PEGDA structure to C – C bonds during gamma irradiation and the formation of covalent bonds between the polymers. Therefore, these results suggested the formation of chemical crosslinking between the PEGDA and alginate as supported by the data from gel fraction, SEM, and mechanical properties analyses.

3.2. CIP release from PEGDA and PEGDA/ALG hydrogels

CIP was incorporated within the PEGDA and PEGDA/ALG hydrogels before hydrogel fabrication, indicating that hydrogel network formation and CIP encapsulation occurred simultaneously during gamma-irradiation. In order to investigate the effect of gamma-irradiation on the CIP structure, UV/Vis spectrum measurements of the released CIP from the

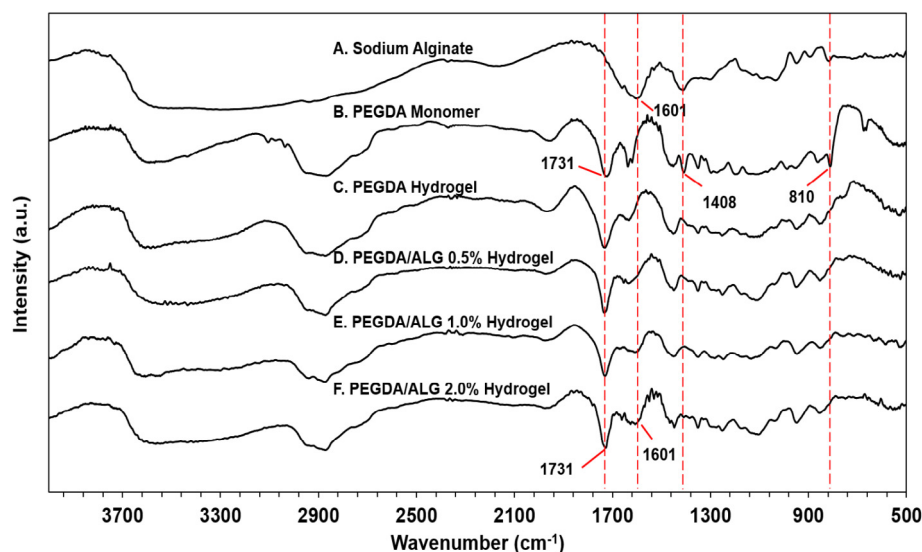


Fig. 5 FTIR spectra of sodium alginate, PEGDA monomer, and PEGDA and PEGDA/ALG hydrogels.

PEGDA/ALG 1.0% hydrogel were conducted. The results showed that the UV/Vis spectrum of the released CIP from the hydrogel was similar to that of free CIP (Fig. 6A). These results suggest that gamma radiation did not disrupt the CIP structure. It has been reported that CIP showed chemical stability after gamma-irradiation doses up to 100 kGy (Al-Mohizea et al., 2007). In addition, the 3D structure of the hydrogels may act as a protective agent, which protects the CIP from harsh environmental conditions and maintains the bioactivity of the encapsulated CIP.

The release profile of encapsulated drugs may take place by several mechanisms such as swelling, diffusion, environmental changes, and drug-matrix interaction (Fan et al., 2020; Li & Mooney, 2016; Rizwan et al., 2017; Zang et al., 2022). To investigate the release profile of the encapsulated CIP from PEGDA and PEGDA/ALG hydrogels, in vitro release of CIP from PEGDA and PEGDA/ALG hydrogels was carried out by incubating the hydrogels in three different pH values, which are pH = 2, pH = 7.4, and pH = 10. The CIP release profiles of the PEGDA and PEGDA/ALG hydrogels at different pH values, as shown in Fig. 6B-D, revealed that all hydrogels showed lower CIP release at an acidic pH (pH = 2) (Fig. 6B), while they exhibited higher CIP release at physiological pH (pH = 7.4) (Fig. 6C) and basic pH (pH = 10) (Fig. 6D). Interestingly, we observed that the alginate content in the hydrogels influenced the percentage of the released CIP. It shows that hydrogel with the highest alginate content (PEGDA/ALG 2.0%) has the fewest CIP releases ($35.08 \pm 4.55\%$) after 240 min incubation in pH 2, while PEGDA hydrogel without alginate shows the largest CIP release ($49.38 \pm 9.46\%$) in pH 2 (Fig. 6B). These results were presumably driven by the pore size of the PEGDA and PEGDA/ALG hydrogels. The PEGDA/ALG 2.0% hydrogel

showed the smallest pore size as revealed by the SEM images and the highest crosslinking density as demonstrated by mechanical property characterization, thus it affects the release ability of the CIP from the hydrogel. It has been reported that pore size in the hydrogel structure plays an important role in deciding their ability to release the drug in physiological fluids in vitro and/or in vivo (Rizwan et al., 2017). The previous report also demonstrated that the drug diffusion coefficient through hydrogels decreases as the cross-linking density increases and as the equilibrium degree of swelling decreases (Canal & Peppas, 1989; Zang et al., 2022).

In addition, the encapsulated CIP may interact with the polymers in the hydrogels via hydrogen bonding. Therefore, it may prevent CIP release. These results were confirmed by the FTIR spectra of the hydrogels, which showed strong intermolecular interactions in the PEGDA/ALG hydrogels containing CIP.

These findings indicate that hydrogels containing alginate can protect CIP better than that PEGDA hydrogel, implying that the PEGDA/ALG hydrogels can be applied as a protective shield to protect CIP from harsh environmental conditions, such as stomach conditions.

3.3. Antibacterial activity of PEGDA and PEGDA/ALG hydrogels containing CIP

Antibacterial activity against *E. coli* and *S. aureus* of the PEGDA and PEGDA/ALG hydrogels containing CIP was investigated using a double-layer diffusion method. After one day of incubation of the hydrogels, the clear zones appeared in the agar medium containing bacteria, indicating the release of CIP from the hydrogels (Fig. 7A-B). The PEGDA hydrogel

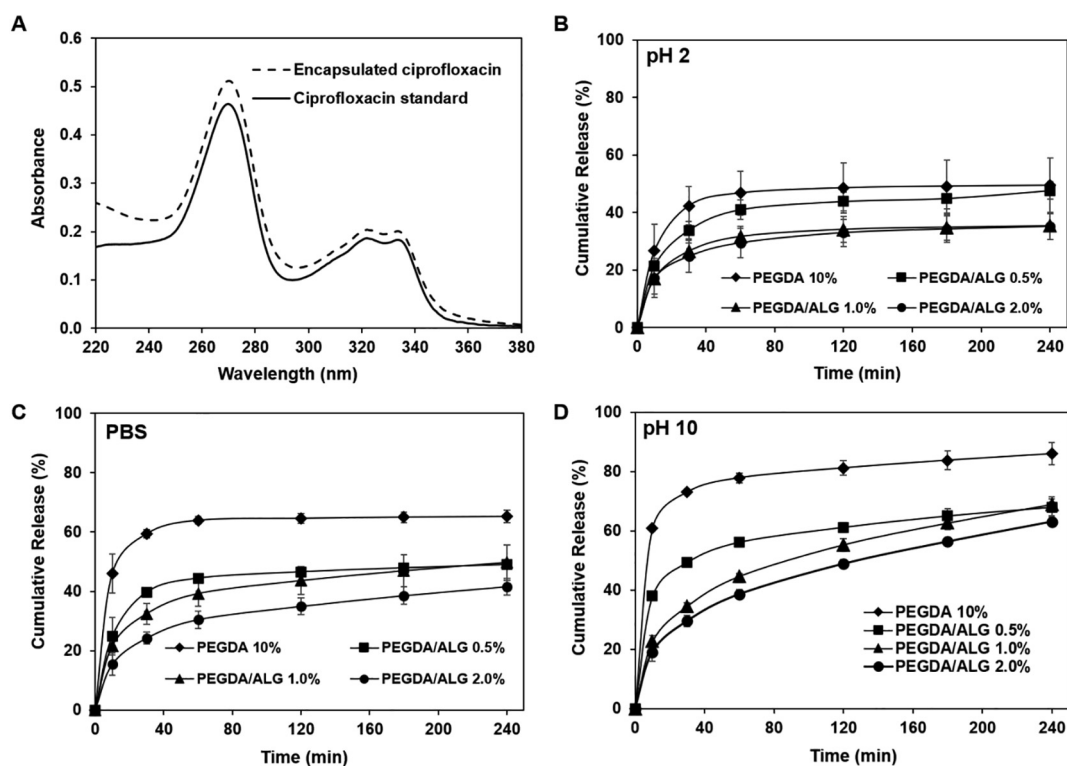


Fig. 6 UV/Vis spectra of free and encapsulated CIP (A), the release profile of CIP from PEGDA/ALG hydrogels at pH 2 (B), PBS (C), and pH 10 (D).

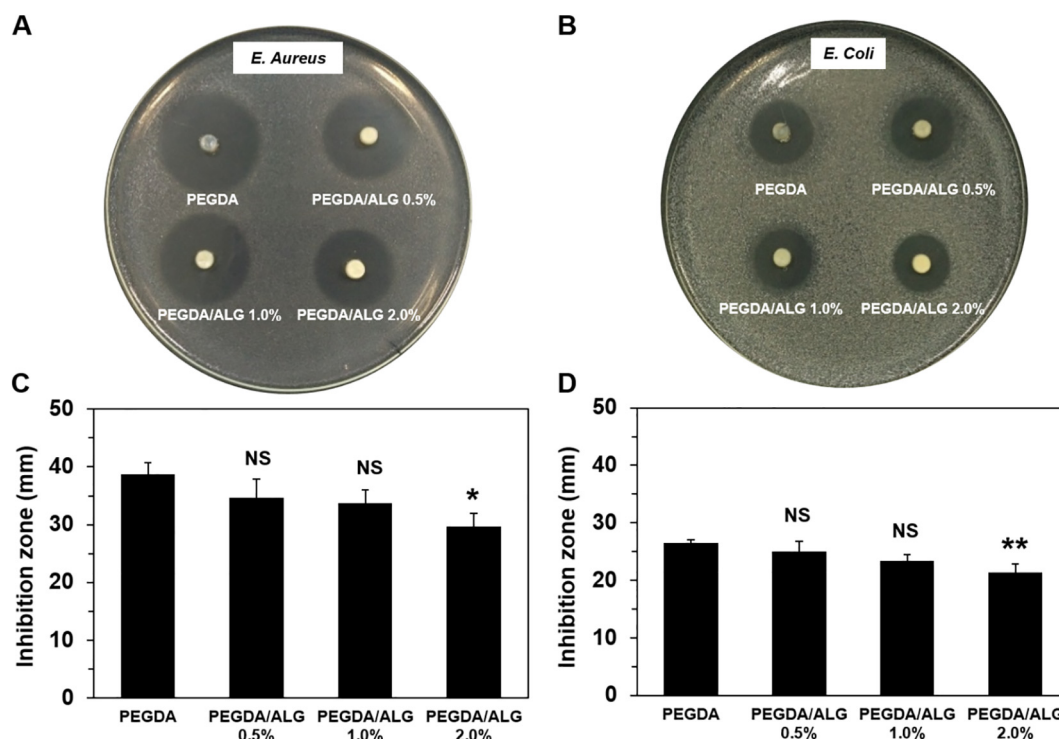


Fig. 7 Antibacterial activity of the PEGDA and PEGDA/ALG hydrogels containing CIP against *S. aureus* (A and C) and *E. coli* (B and D) (* $p < 0.05$; ** $p < 0.01$; and NS = Not significant compared to PEGDA hydrogel).

exhibited a better performance in antibacterial activity against the *S. aureus* and *E. coli* compared to those PEGDA/ALG hydrogels (Fig. 7C-D). These results are in agreement with the results from in vitro release of the CIP from the hydrogels at different pH values, indicating that the degree of crosslinking may influence the ability of the hydrogels to release the CIP. Hydrogels with lower degree of crosslinking or higher pore size released more CIP and were more active against the bacteria. These results indicate that the pore size of the hydrogels can control the CIP release from the hydrogels.

4. Conclusion

Gamma-irradiation has been successfully used to simultaneously encapsulate CIP into PEGDA and PEGDA/ALG hydrogels. SEM images exhibited a porous structure of the hydrogels, and the pore size of the hydrogels decreases with increasing alginate concentration. The gel fraction and FT-IR spectra analyses of the PEGDA/ALG hydrogels indicated the crosslinking formation between alginate and PEGDA in the hydrogels. Drug stability and release experiments using a UV/Vis spectrophotometer showed that the CIP in the hydrogels was stable and showed a sustained release profile. Furthermore, this study revealed that the PEGDA/ALG hydrogels can control CIP release better than the PEGDA hydrogel, implying that the PEGDA/ALG hydrogels have the potential as 3D scaffolds for CIP delivery due to their ease of fabrication, ability to control CIP release, and support CIP bioactivity.

CRedit authorship contribution statement

Farah Nurlidar: Conceptualization, Supervision, Investigation, Methodology, Data curation, Formal analysis, Validation, Visualization, Writing – original draft, Writing – review &

editing. **Dien Puji Rahayu:** Methodology, Data curation, Writing - review & editing. **Deudeu Lasmawati:** Writing – review & editing, Investigation, Methodology, Data curation. **Ade Les-tari Yunus:** Writing – review & editing, Investigation, Methodology, Data curation. **Rika Heryani:** Writing – review & editing, Investigation, Methodology, Data curation. **Nani Sur-yani:** Writing – review & editing, Investigation, Methodology, Data curation.

Declaration of Competing Interest

The authors declare that they have no known competing financial interests or personal relationships that could have appeared to influence the work reported in this paper.

Acknowledgements

This work was supported in part by the DIPA (2019) of the Center for Radiation and Isotope Applications, National Nuclear Energy Agency. The authors acknowledge Dr. Mime Kobayashi from Nara Institute of Science and Technology, Japan, for the gift of sodium alginate and ciprofloxacin. The authors also acknowledge Ms. Fajar Lukitowati for providing the bacteria used in the antibacterial test.

References

- Ailincăi, D., Agop, M., Marinas, I.C., Zala, A., Irimiciuc, S.A., Dobreci, L., Petrescu, T.C., Volovat, C., 2021. Theoretical model for the diclofenac release from PEGylated chitosan hydrogels. *Drug Deliv.* 28 (1), 261–271. <https://doi.org/10.1080/10717544.2021.1876181>.

- Al-Mohizea, A.M., El-Bagory, I.M., Alsarra, I.A., Al-Jenoobi, F.I., Bayomi, M.A., 2007. Effect of gamma radiation on the physico-chemical properties of ciprofloxacin in solid state. *J. Drug Delivery Sci. Technol.* 17 (3), 211–215. [https://doi.org/10.1016/S1773-2247\(07\)50038-9](https://doi.org/10.1016/S1773-2247(07)50038-9).
- Bakaic, E., Smeets, N.M.B., Hoare, T., 2015. RSC Advances and derivatives as functional biomaterials. *RSC Adv.* 5, 35469–35486. <https://doi.org/10.1039/C4RA13581D>.
- Bignotti, F., Baldi, F., Grassi, M., Abrami, M., Spagnoli, G., 2021. Hydrophobically-modified PEG hydrogels with controllable hydrophilic/hydrophobic balance. *Polymers* 13 (9). <https://doi.org/10.3390/polym13091489>.
- Bustamante-Torres, M., Pino-Ramos, V.H., Romero-Fierro, D., Hidalgo-Bonilla, S.P., Magaña, H., Bucio, E., 2021. Synthesis and antimicrobial properties of highly cross-linked pH-sensitive hydrogels through Gamma radiation. *Polymers* 13 (14). <https://doi.org/10.3390/polym13142223>.
- Canal, T., Peppas, N.A., 1989. Correlation between mesh size and equilibrium degree of swelling of polymeric networks. *J. Biomed. Mater. Res.* 23 (10), 1183–1193. <https://doi.org/10.1002/jbm.820231007>.
- D'souza, A.A., Shegokar, R., 2016. Polyethylene glycol (PEG): a versatile polymer for pharmaceutical applications. *Expert Opin. Drug Deliv.* 13 (9), 1257–1275. <https://doi.org/10.1080/17425247.2016.1182485>.
- Dahri, M., Akbarialiabadi, H., Jahromi, A.M., Maleki, R., 2021. Loading and release of cancer chemotherapy drugs utilizing simultaneous temperature and pH-responsive nanohybrid. *BMC Pharmacol. Toxicol.* 22 (1), 1–10. <https://doi.org/10.1186/s40360-021-00508-8>.
- Darwis, D., Erizal, Abbas, B., Nurlidar, F., & Putra, D. P. (2015). Radiation Processing of Polymers for Medical and Pharmaceutical Applications. *Macromolecular Symposia*, 353(1), 15–23. 10.1002/masy.201550302
- Das, S., Kumar, V., Tiwari, R., Singh, L., & Singh, S. (2018). Recent Advances in Hydrogels for Biomedical Applications. *Asian Journal of Pharmaceutical and Clinical Research*, 11(11), 62. 10.22159/ajpcr.2018.v11i11.27921.
- El-Bagory, I.M., Bayomi, M.A., Mahrous, G.M., Alanazi, F.K., Alsarra, I.A., 2010. Effect of gamma irradiation on pluronic gels for ocular delivery of ciprofloxacin: In vitro evaluation. *Aust. J. Basic Appl. Sci.* 4 (9), 4490–4498.
- Fan, Z., Cheng, P., Liu, M., Prakash, S., Han, J., Ding, Z., Zhao, Y., Wang, Z., 2020. Dynamic crosslinked and injectable biohydrogels as extracellular matrix mimics for the delivery of antibiotics and 3D cell culture. *RSC Adv.* 10 (33), 19587–19599. <https://doi.org/10.1039/d0ra02218g>.
- Fekete, T., Borsá, J., Takács, E., Wojnárovits, L., 2017. Synthesis of carboxymethylcellulose/starch superabsorbent hydrogels by gamma-irradiation. *Chem. Cent. J.* 11 (1), 1–11. <https://doi.org/10.1186/s13065-017-0273-5>.
- Hanna, D.H., Saad, G.R., 2019. Encapsulation of ciprofloxacin within modified xanthan gum- chitosan based hydrogel for drug delivery. *Bioorg. Chem.* 84 (October 2018), 115–124. <https://doi.org/10.1016/j.bioorg.2018.11.036>.
- Henise, J., Hearn, B.R., Ashley, G.W., Santi, D.V., 2015. Biodegradable tetra-peg hydrogels as carriers for a releasable drug delivery system. *Bioconjug. Chem.* 26 (2), 270–278. <https://doi.org/10.1021/bc5005476>.
- Jonah, C.D., Spinks, J.W.T., Woods, R.J., 1990. Introduction to radiation chemistry. *Radiat. Res.* 124 (3), 378. <https://doi.org/10.2307/3577852>.
- Khan, Y.A., Ozaltin, K., Bernal-Ballen, A., Di Martino, A., 2021. Chitosan-alginate hydrogels for simultaneous and sustained releases of ciprofloxacin, amoxicillin and vancomycin for combination therapy. *J. Drug Delivery Sci. Technol.* 61. <https://doi.org/10.1016/j.jddst.2020.102126>.
- Li, J., & Mooney, D. J. (2016). Designing hydrogels for controlled drug delivery. In *Nature Reviews Materials* (Vol. 1, Issue 12). Nature Publishing Group. 10.1038/natrevmats.2016.71.
- Liu, L., Yao, W.D., Rao, Y.F., Lu, X.Y., Gao, J.Q., 2017. pH-responsive carriers for oral drug delivery: challenges and opportunities of current platforms. *Drug Deliv.* 24 (1), 569–581. <https://doi.org/10.1080/10717544.2017.1279238>.
- Mahmood, A., Patel, D., Hickson, B., Desrochers, J., Hu, X., 2022. Recent progress in biopolymer-based hydrogel materials for biomedical applications. *Int. J. Mol. Sci.* 23 (3). <https://doi.org/10.3390/ijms23031415>.
- Mantha, S., Pillai, S., Khayambashi, P., Upadhyay, A., & Zhang, Y. (2019). Smart Hydrogels in Tissue Engineering and. *Materials*, 12 (3323), 33. <https://www.ncbi.nlm.nih.gov/pmc/articles/PMC68/>
- Masyuroh, S. F., Deudeu, L., Suryani, N., Sumarlin, L. O., & Nurlidar, F. (2020). Release of ciprofloxacin from gamma-irradiated PEGDA-chitosan hydrogel. *AIP Conference Proceedings*, 2296. <https://aip.scitation.org/doi/abs/10.1063/5.0030348>.
- Nagasawa, N., Mitomo, H., Yoshii, F., Kume, T., 2000. Radiation-induced degradation of sodium alginate. *Polym. Degrad. Stab.* 69 (3), 279–285. [https://doi.org/10.1016/S0141-3910\(00\)00070-7](https://doi.org/10.1016/S0141-3910(00)00070-7).
- Nho, Y.C., Park, J.S., Shin, J.W., Lim, Y.M., Jeong, S.I., Shin, Y.M., Gwon, H.J., Khil, M.S., Lee, D.W., Ahn, S.J., 2015. Poly(acrylic acid)/polyethylene glycol hydrogel prepared by using gamma-ray irradiation for mucosa adhesion. *J. Korean Phys. Soc.* 66 (1), 17–21. <https://doi.org/10.3938/jkps.66.17>.
- Norioka, C., Inamoto, Y., Hajime, C., Kawamura, A., & Miyata, T. (2021). *A universal method to easily design tough and stretchable hydrogels*. 10.1038/s41427-021-00302-2
- Nurlidar, F., Kobayashi, M., Terada, K., Ando, T., Tanihara, M., 2017. Cytocompatible polyion complex gel of poly(Pro-Hyp-Gly) for simultaneous rat bone marrow stromal cell encapsulation. *J. Biomater. Sci. Polym. Ed.* 28 (14), 1480–1496. <https://doi.org/10.1080/09205063.2017.1331872>.
- Nurlidar, F., Yamane, K., Kobayashi, M., Terada, K., Ando, T., Tanihara, M., 2018. Calcium deposition in photocrosslinked poly (Pro-Hyp-Gly) hydrogels encapsulated rat bone marrow stromal cells. *J. Tissue Eng. Regen. Med.* 12 (3), e1360–e1369. <https://doi.org/10.1002/term.2520>.
- Nurlidar, F., Kobayashi, M., Yunus, A.L., Yunus, M.Y., Puspitasari, T., Darwis, D., 2022. Gamma-irradiated bacterial cellulose as a three-dimensional scaffold for osteogenic differentiation of rat bone marrow stromal cells. *Indonesian J. Chem.* 22 (3), 816–826. <https://doi.org/10.22146/ijc.71823>.
- Park, J., Kim, M., Choi, S., Sun, J.Y., 2020. Self-healable soft shield for γ -ray radiation based on polyacrylamide hydrogel composites. *Sci. Rep.* 10 (1), 1–8. <https://doi.org/10.1038/s41598-020-78663-x>.
- Rizwan, M., Yahya, R., Hassan, A., Yar, M., Azzahari, A.D., Selvanathan, V., Sonsudin, F., Abouloula, C.N., 2017. pH sensitive hydrogels in drug delivery: brief history, properties, swelling, and release mechanism, material selection and applications. *Polymers* 9 (4). <https://doi.org/10.3390/polym9040137>.
- Tomić, S.L., Mičić, M.M., Filipović, J.M., Suljovrujić, E.H., 2007. Swelling and drug release behavior of poly(2-hydroxyethyl methacrylate/itaconic acid) copolymeric hydrogels obtained by gamma irradiation. *Radiat. Phys. Chem.* 76 (5), 801–810. <https://doi.org/10.1016/j.radphyschem.2006.05.013>.
- Visentini, A.F., Dong, T., Poli, J., Panzer, M.J., 2014. Rapid, microwave-assisted thermal polymerization of poly(ethylene glycol) diacrylate-supported ionogels. *J. Mater. Chem. A* 2 (21), 7723–7726. <https://doi.org/10.1039/c4ta00907j>.
- Wang, Y., Wang, J., Yuan, Z., Han, H., Li, T., Li, L., Guo, X., 2017. Chitosan cross-linked poly(acrylic acid) hydrogels: Drug release control and mechanism. *Colloids Surf. B Biointerfaces* 152, 252–259. <https://doi.org/10.1016/j.colsurfb.2017.01.008>.
- Yoo, M.K., Kweon, H.Y., Lee, K.G., Lee, H.C., Cho, C.S., 2004. Preparation of semi-interpenetrating polymer networks composed

- of silk fibroin and poloxamer macromer. *Int. J. Biol. Macromol.* 34 (4), 263–270. <https://doi.org/10.1016/j.ijbiomac.2004.06.002>.
- Zang, Z., Zhao, S., Yang, M., Yu, C., Ouyang, H., Chen, L., Zhu, W., Liao, Z. gen, Naeem, A., & Guan, Y. (2022). Blood chemical components analysis of honeysuckle and formulation of xanthan gum/starch-based (PVA-co-AA) hydrogels for controlled release. *Arabian Journal of Chemistry*, 15(12), 104312. 10.1016/j.arabjc.2022.104312
- Zhang, Y., Yu, T., Peng, L., Sun, Q., Wei, Y., & Han, B. (2020). Advancements in Hydrogel-Based Drug Sustained Release Systems for Bone Tissue Engineering. In *Frontiers in Pharmacology* (Vol. 11). Frontiers Media S.A. 10.3389/fphar.2020.00622.